ELSEVIER

Polymer 43 (2002) 1983–1992

polymer

www.elsevier.com/locate/polymer

Copolyimides with trifluoromethyl or methoxy substituents. NMR characterization

Eliette Pinel[a], Corine Bas[a,*], Sylvie Neyertz[a], N. Dominique Albérola[a], Roger Petiaud[b], Regis Mercier[c]

[a]*Laboratoire Matériaux Organiques à Propriétés Spécifiques (LMOPS), UMR 5041, Université de Savoie, Bâtiment IUT, Campus Scientifique, 73376 Le Bourget-du-Lac Cedex, France*

[b]*Service Central d'Analyse (SCA), BP 22, 69390 Vernaison, France*

[c]*Laboratoire Matériaux Organiques à Propriétés Spécifiques (LMOPS), UMR 5041, Université de Savoie, BP 24, 69390 Vernaison, France*

Received 28 October 2001; received in revised form 13 December 2001; accepted 20 December 2001

Abstract

In the first stage, a series of aromatic diamine compounds such as 2-methoxy-5,4′-diaminodiphenyl ether (ODAOMe) and 2-trifluomethyl-4,4′-diaminodiphenyl ether ($ODACF_3$) were synthesized. These aromatic diamines and 4,4′-diaminodiphenyl ether (ODA) were then used to prepare copolyimides with 4,4′-oxydiphthalic anhydride (ODPA) and bicyclo[2.2.2]-oct-7-ene-2,3,5,6-tetracarboxylic dianhydride (BCDA). Both chemical composition and the arrangements of repetitive units were characterized by ^{1}H and ^{19}F NMR. It was shown that solubility and thermal stability are related to the BCDA fraction in the copolymers and to the chemical structure of the diamine.

Keywords: Copolymer synthesis; Alicyclic dianhydride; NMR characterization

1. Introduction

It is well known that aromatic polyimides offer a combination of outstanding properties such as chemical and thermal stabilities, electrical and mechanical properties, gas separation characteristics, etc. [1]. Some of these properties can be tailored by modifying either the chemical structure of the main chain or that of the substituents [2–4]. Another approach is to synthesize random, alternating or block copolyimides with either a diamine and different dianhydrides or a dianhydride and different diamines [5–10].

In most cases, polyimide solubility is required for processing. According to the literature [11–13], polyimides based on bicyclo[2.2.2]-oct-7-ene-2,3,5,6-tetracarboxylic dianhydride (BCDA) are soluble in most common solvents but their thermal stability is lowered due to the aliphatic character of the BCDA fragment. In contrast, polyimides based on 4,4′-oxydiphthalic anhydride (ODPA) show low glass transition temperature, high degradation temperatures but rather low solubilities [14].

In this work, we have synthesized copolyimides based on both ODPA and BCDA dianhydrides. These dianhydrides were reacted with 2-methoxy-5,4′-diaminodiphenyl ether (ODAOMe), 2-trifluomethyl-4,4′-diaminodiphenyl ether ($ODACF_3$) or 4,4′-diaminodiphenyl ether (ODA). As the chemical structure of end groups affects the properties of the polyimide [15,16], all copolyimides were end-capped using 4-*tert*-butyl phthalic anhydride (PAtBu). The resulting polyimides were thoroughly characterized by NMR. Thermal properties and solvent resistances were also evaluated.

2. Experimental section

2.1. Materials

2.1.1. Reagents and solvents

Bicyclo[2.2.2]-oct-7-ene-2,3,5,6-tetracarboxylic dianhydride (BCDA), 4,4′-oxydiphthalic anhydride (ODPA) and the 4,4′-diaminodiphenyl ether (ODA) were purchased from Aldrich Chemical Co. and purified by vacuum sublimation. The different solvents, dimethyl formamide (99%), ethyl acetate (99.5%) and *m*-cresol (99%) were purchased from Merck and used without further purification.

* Corresponding author. Tel.: +33-479-75-86-24; fax: +33-479-75-86-14.

E-mail address: corine.bas@univ-savoie.fr (C. Bas).

0032-3861/02/$ - see front matter
PII: S0032-3861(02)00004-6

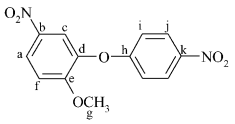

2-methoxy-5,4'-dinitrodiphenyl ether

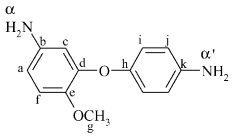

2-methoxy-5,4'-diaminodiphenyl ether (ODAOMe)

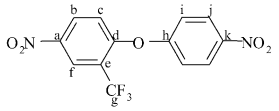

2-trifluomethyl-4,4'-dinitrodiphenyl ether

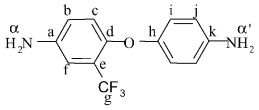

2-trifluomethyl-4,4'-diaminodiphenyl ether ($ODACF_3$)

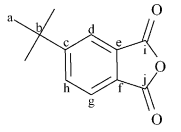

4-tertiobutyl phtalic anhydride (PAtBu)

Fig. 1. Structure of synthesized compounds.

2.1.2. Syntheses of the monomers (Fig. 1)

2.1.2.1. Synthesis of 2-methoxy-5,4′-dinitrodiphenyl ether. In a three-necked round-bottomed flask fitted with a nitrogen inlet tube and a reflux condenser, a mixture of 15.09 g (8.93×10^{-2} mol) of 2-methoxy-5-nitrophenol, 14.52 g (9.28×10^{-2} mol) of 4-chloronitrobenzene, 50 ml of dimethyl formamide and 13.67 g (9.9×10^{-2} mol) of potassium carbonate was heated at 120 °C for 5 h. The mixture was then poured into a sodium hydroxide water solution (20 g/l). The precipitate was filtered off and dried in a vacuum oven. The imide product was purified by recrystallization in isopropanol (66% yield).

Mp: 127 °C; RMN ^{1}H (250 MHz, DMSO-d_6) 3.90 ppm (s, 3H, H_g); 7.13 ppm (d, $^3J_{HH} = 9.1$ Hz; 2H, H_i); 7.48 ppm (d, $^3J_{HH} = 9.1$ Hz; 1H, H_f); 8.12 ppm (d, $^4J_{HH} = 2.7$ Hz; 1H, H_c); 8.23 ppm (d, $^3J_{HH} = 9.1$ Hz; 2H; H_j); 8.30 ppm (dd, $^4J_{HH} = 2.7$ Hz; $^3J_{HH} = 9.1$ Hz; 1H, H_a); RMN ^{13}C (62.9 MHz, DMSO-d_6) 56.8 ppm (1C, C_g); 113.6 ppm (1C, C_f); 116.5 ppm (2C, C_i); 117.9 ppm (1C, C_b or C_k); 123.0 ppm (1C, C_c); 125.9 ppm (2C, C_j); 140.9 ppm (1C, C_b or C_k); 141.9 ppm (1C, C_k); 142.7 ppm (1C, C_d); 157.0 ppm (1C, C_e); 162.1 ppm (1C, C_h).

2.1.2.2. Synthesis of 2-methoxy-5,4′-diaminodiphenyl ether (ODAOMe). In a three-necked round-bottomed flask equipped with a nitrogen inlet and a reflux condenser, 2-methoxy-5,4′-dinitrodiphenyl ether was introduced with Pd/C as catalyst in ethyl acetate. Hydrazine was then added dropwise to the solution while keeping the temperature around 35 °C. After complete addition of the hydrazine, the mixture was stirred at 60 °C for 4 h. The catalyst was separated from the mixture by filtration over Celite® and the solvent was evaporated. The residue was purified by washing first in isopropanol followed by a wash in ether (90% yield).

Mp: 103 °C; RMN ^{1}H (250 MHz, DMSO-d_6) 3.63 ppm (s, 3H, H_g); 4.54 ppm (s, 2H, $H_{\alpha'}$); 4.66 ppm (s, 2H, H_α); 6.10 ppm (d, $^4J_{HH} = 2.5$ Hz; 1H, H_c); 6.22 ppm (dd, $^4J_{HH} = 2.5$ Hz; $^3J_{HH} = 8.4$ Hz; 1H, H_a); 6.55 ppm (d, $^3J_{HH} = 8.6$ Hz; 2H, H_i); 6.66 ppm (d, $^3J_{HH} = 8.6$ Hz; 2H, H_j); 6.75 ppm (d, $^3J_{HH} = 8.4$ Hz; 1H, H_f); RMN ^{13}C (62.9 MHz, DMSO-d_6) 62.4 ppm (1C, C_g); 110.8 ppm (1C, C_f); 113.6 ppm (2C, C_i); 120.2 ppm (1C, C_a); 121.4 ppm (1C, C_c); 124.3 ppm (2C, C_j); 146.8 ppm (1C, C_k or C_b); 148.7 ppm (1C, C_b or C_k); 149.4 ppm (1C, C_d or C_h); 152.8 ppm (1C, C_e); 153.3 ppm (1C, C_h or C_d).

2.1.2.3. Synthesis of 2-trifluomethyl-4,4′-dinitrodiphenyl ether. 20.06 g (0.089 mol) of 2-chloro-5-nitrotrifluomethylbenzene and 14.02 g (0.10 mol) of 4-nitrophenol as well as 50 ml of dimethylformamide and 14.70 g (0.11 mol) of potassium carbonate were introduced in a three-necked flask. The solution was stirred at 60 °C for 6 h. This mixture was then poured into a solution of NaOH (20 g/l). The solid was filtered off and dried (95% yield).

Mp: 83 °C; RMN ^{1}H (250 MHz, DMSO-d_6) 7.45 ppm (m, 3H, H_{i+c}); 8.35 ppm (d, $^3J_{HH} = 9.1$ Hz; 2H, H_j); 8.38 ppm (d, $^3J_{HH} = 2.1$ Hz; 1H, H_f); 8.52 ppm (dd, $^3J_{HH} = 9.1$ Hz; $^3J_{HH} = 2.1$ Hz; 1H, H_b); RMN ^{13}C (62.9 MHz, DMSO-d_6) 119.9 ppm (1C, C_c); 120.2 ppm (2C, C_i); 120.3 ppm (q, $^2J_{CF} = 32$ Hz; 1C, C_e); 122.7 ppm (q, $^1J_{CF} = 200$ Hz; 1C, C_g); 123.7 ppm (q, $^3J_{CF} = 4.6$ Hz; 1C, C_f); 126.6 ppm (2C, C_j); 130.4 ppm (1C, C_b); 143.4 ppm (1C, C_k or C_a); 144.5 ppm (1C, C_a or C_k); 158.0 ppm (1C, C_h); 160.0 ppm (1C, C_d).

2.1.2.4. Synthesis of 2-trifluomethyl-4,4′-diaminodiphenyl ether ($ODACF_3$). The 2-trifluomethyl-4,4′-dinitrodiphenyl ether was dissolved in ethyl acetate and Pd/C catalyst was added to the reactor. The solution was stirred under

hydrogen flow at 35 °C for 4 h. The solution was filtered and the solvent was evaporated (68% yield).

Mp: 111 °C; RMN ^{1}H (250 MHz, DMSO-d_6) 4.87 ppm (s, 2H, $H_{\alpha'}$); 5.25 ppm (s, 2H, H_{α}); 6.53 ppm (d, $^{3}J_{HH} = 8.9$ Hz; H_i); 6.64 ppm (d, $^{3}J_{HH} = 8.9$ Hz; 2H, H_j); 6.66 ppm (d, $^{3}J_{HH} = 8.6$ Hz; 1H; H_c); 6.74 ppm (dd, $^{3}J_{HH} = 2.5$ Hz; $^{3}J_{HH} = 8.6$ Hz; 1H, H_b); 6.86 ppm (d, $^{3}J_{HH} = 2.5$ Hz; 1H, H_f); RMN ^{13}C (62.9 MHz, DMSO-d_6) 110.8 ppm (q, $^{3}J_{CF} = 5.5$ Hz; 1C, C_f); 114.9 ppm (2C, C_j); 118.8 ppm (1C, C_c or C_b); 119.2 ppm (2C, C_i); 119.9 ppm (q, $^{2}J_{CF} = 29.6$ Hz; 1C, C_e); 123.9 ppm (q, $^{1}J_{CF} = 272$ Hz; 1C, C_g); 129.8 ppm (1C, C_b or C_c); 144.4 ppm (1C, C_k or C_a); 144.8 ppm (1C, C_a or C_k); 145.5 ppm (1C, C_d); 148.0 ppm (1C, C_h).

2.1.2.5. Synthesis of 4-tert-butyl phthalic anhydride (PAtBu). A mixture containing 15.0 g (9.3×10^{-2} mol) *tert*-butyl-*o*-xylene, 40 ml of pyridine and 100 ml of water was placed in a three-necked round-bottomed flask and heated at 90 °C. A total (0.44 mol) of 70.0 g potassium permanganate was added to the stirred mixture over an interval of 3 h. After 1 h, the magnesium dioxide was removed from the mixture by filtration. The filtrate was then concentrated and acidified with hydrochloric acid. The precipitate was filtered and placed at the reflux in acetic anhydride for 2 h. The warm solution was filtered to remove pyridinium salts. The desired compound was isolated by evaporating the acetic anhydride under vacuum. It was recrystallized in ether to yield a white powder (72% yield).

IR (cm^{-1}): 1849, 1774 (anhydride); RMN ^{1}H (250 MHz, DMSO-d_6 anhydride) 1.41 ppm (s, 9H, H_a); 7.92 ppm (m, 2H, H_{d+g}); 8.01 ppm (m, 1H, H_h); RMN ^{13}C (62.9 MHz, DMSO-d_6 anhydre) 31.0 ppm (3C, C_a); 36.1 ppm (1C, C_b); 122.6 ppm (1C, C_d or C_g); 125.5 ppm (1C, C_g or C_d); 128.5 ppm (1C, C_e); 131.6 ppm (1C, C_f); 133.5 ppm (1C, C_h); 161.2 ppm (1C, C_c); 162.8 ppm (1C, C_j or C_i); 163.3 ppm (1C, C_j or C_i).

2.2. General procedure for polymerization

2.2.1. Syntheses of the homopolymers

The dianhydride (ODPA or BCDA), the diamine (ODA, ODAOMe or $ODACF_3$) and the end-capped monomer (PAtBu) as well as the solvent (*m*-cresol) were added simultaneously in a three-necked flask, under nitrogen atmosphere. The mass of each monomer was calculated in order to have a molecular weight of polymer of about 20,000 g/mol. For example, for the ODA-0 homopolyimide, the amounts were 3.0246 g (0.00975 mol) of ODPA dianhydride, 2.0000 g (0.0100 mol) of ODA diamine and 0.0973 g (0.0005 mol) of PAtBu monoanhydride. The solid concentration was set to 20 wt%. The reaction solution was first stirred at 100 °C for complete dissolution of the reagents and then at 180 °C for 5 h, under nitrogen. After cooling down, the solution was poured into methanol. The precipitate was filtered and dried under reduced pressure for 24 h at 100 °C.

2.2.2. Syntheses of the copolymer

The syntheses of copolyimides were carried out under conditions similar to those of the homopolymers, but in a two-step procedure. The amount of each monomer was calculated as a function of the content of each dianhydride and of the molar weight of the polymer. In a typical example of ODAOMe-20, to a 100 ml flask, 2.0000 g (0.00869 mol) of ODAOMe diamine were first dissolved in *m*-cresol with 2.1022 g (0.00678 mol) of ODPA dianhydride. After complete dissolution at 100 °C and stirring for 5 h at 180 °C under nitrogen, the solution was cooled down. In a second step, 0.4205 g (0.00169 mol) of BCDA dianhydride and 0.0878 g (0.00043 mol) of the end-capped monomer (PAtBu) were added to the solution. The total diamine/dianhydride concentration in *m*-cresol was maintained at 20 wt%. The reaction was then allowed to continue at 180 °C for 5 h under nitrogen. After cooling down, the solution was poured into methanol. The precipitate was filtered and dried under reduced pressure for 24 h at 100 °C. Copolyimides with different mole ratios based on different diamines were synthesized in a similar way.

2.3. Measurements

The proton and carbon-13 NMR spectra of the monomers were obtained using a Bruker AC 250 MHz, with $CDCl_3$, CD_2Cl_2 or DMSO-d_6 as solvents. The proton, carbon-13 NMR and fluorine-19 NMR spectra of polyimide films were recorded on a Bruker DR400 using $CDCl_3$ as a solvent. Tetramethylsilane (TMS) was used as reference for proton NMR and fluoroform for fluorine-19 NMR. ^{19}F NMR chemical shifts were evaluated using trifluoroacetic acid as an internal standard whose chemical shift is −78.5 ppm.

The Fourier transform infrared spectra (IRTF) were recorded on a Perkin Elmer Paragon 1000 spectrophotometer in diffuse reflection mode from the polymer powders.

The solubility of polymers in various organic solvents (1 wt%) was evaluated visually either at room temperature or on heating.

Inherent viscosity measurements were carried out using an Ubbelhode viscosimeter with 0.5 g/dl of polymer dissolved in NMP at 30 °C.

Thermal analyses of polymers were performed using (i) a Perkin Elmer DSC-7 instrument at a heating rate of 20 °C/min under nitrogen atmosphere and (ii) a TA2050—TGA at a heating rate of 5 °C/min both under nitrogen or under air.

3. Results and discussion

3.1. Syntheses of the monomers

The $ODACF_3$ and ODAOMe molecules were prepared in two steps according to Scheme 1. The intermediate dinitro

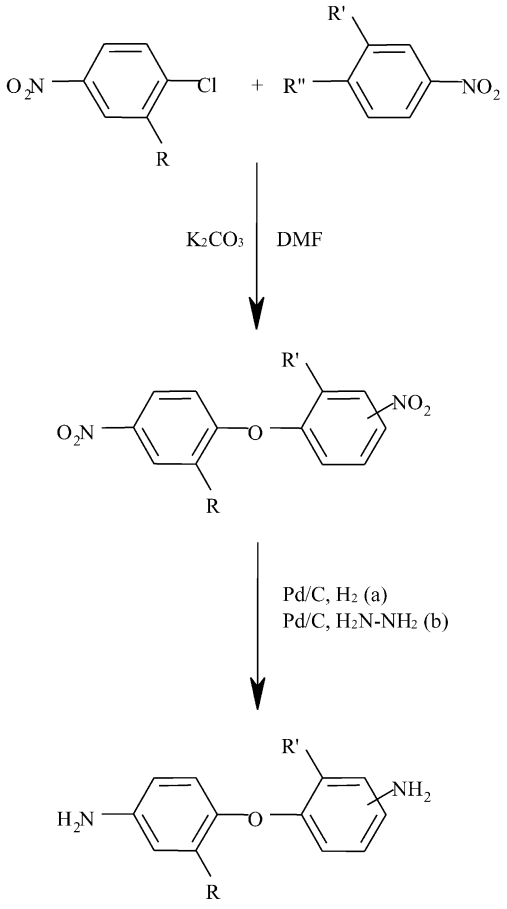

(a) R=CF_3, R'=H, R"=OH
(b) R=H, R'=OH, R"=OCH_3

Scheme 1.

compounds were synthesized via nucleophilic aromatic substitution by reacting 2-chloro-5-nitrotrifluomethylbenzene with 4-nitrophenol, and 2-methoxy-5-nitrophenol with 4-chloronitrobenzene, respectively, in the presence of anhydrous potassium carbonate in DMF. The diamine ODAOMe was obtained by reduction of the nitro groups using hydrazine and Pd/C. Although the dinitro conversion to diamine $ODACF_3$ can also be made with $SnCl_2$ and HCl [14], the reduction reaction involving hydrogen and Pd/C conditions was preferred to obtain the diamine $ODACF_3$. The synthesized diamines were characterized by thin layer chromatography and by ^1H and ^{13}C NMR analyses.

The monoanhydride 4-*tert*-butyl phthalic (PAtBu) was obtained by oxidation of *tert*-butyl-*o*-xylene using potassium permanganate (Scheme 2). The resulting dicarboxylic acid intermediate was cyclized into anhydride by refluxing in acetic anhydride. The PAtBu structure was confirmed by FTIR and NMR.

3.2. Syntheses of the polymers

The polyimides were prepared by polycondensation in *m*-cresol. According to Tamagna et al. [17], *m*-cresol does accelerate the amic acid cyclization into imide. The molecular weight of polymers was controlled to be close to 20,000 g/mol using PAtBu as an end-capped reagent.

As far as homopolyimides are concerned, all monomers involved were added at the same time in the solution. The introduction of PAtBu at the beginning or at the end of the polymerization did not seem to have an effect on the molecular weight as determined by NMR and SEC.

In order to generate copolyimides with a good dispersion of the BCDA groups within the chains, we have limited the BCDA fraction to 20% of the molar quantities of the dianhydrides. Moreover, as the BCDA dianhydride displays a higher reactivity towards imidization reaction than the ODPA dianhydride [17], the synthesis procedure was chosen to avoid competitive reaction of both dianhydrides with the diamines. The copolyimides were thus synthesized in one pot two-step process (Scheme 3). In a first stage, the ODPA dianhydride reacted with an excess of diamine to form diamine-terminated imide oligomers. Then, both BCDA and PAtBu monomers were added to react with the diamine oligomer end-groups. All polyimides which have been synthesized are detailed in Table 1. Complete imidization of the polymers was confirmed by the absence of peaks corresponding to amide and carboxylic acid functions both in NMR and FTIR spectra.

3.3. Characterization of the polymers

The average molecular weight and the BCDA fraction incorporated into the polymer chains were determined from proton NMR. As an example, Fig. 2 shows the ^1H NMR spectrum of the ODA-20 copolyimide. The molar fraction of BCDA was calculated using the integrals of the peaks given by aliphatic and ethylenic BCDA protons as well as aromatic H_6 of ODPA. As reported in Table 2, the results are very close to theoretical values. In order to determine molecular weights, we have assumed that all chains are end-capped with PAtBu groups. Table 2 shows that the obtained values are close to the target value of 20,000 g/mol.

To go further into the chemical characterization of the

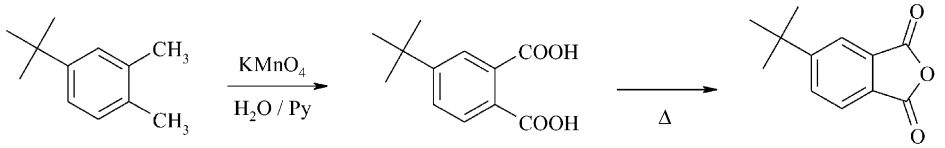

Scheme 2.

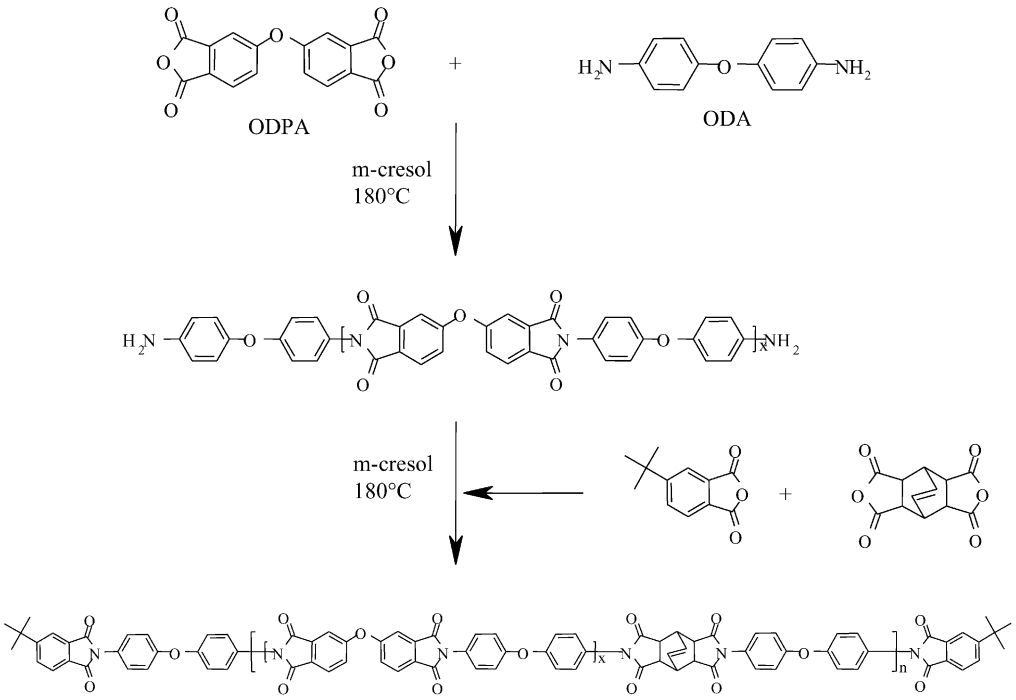

Scheme 3.

copolyimide backbone, we have also carried out FTIR and proton NMR analyses on the oligoimide obtained in the first step.

3.3.1. Copolyimides based on the ODA diamine

The ODPA–ODA oligomer spectrum shows characteristic bands of the imide rings and the diamine functions (ν(C=O): 1777, 1715 cm^{-1}; ν(C–N): 1375 cm^{-1}; $\nu(NH_2)$: 3475, 3368 cm^{-1}). On the other hand, no anhydride band (ν(C=O): 1850, 1770 cm^{-1}) was detected. By comparing the ODPA H_6 and the other aromatic proton signals, the molar ODPA/ODA ratio was determined according Eq. (1). The error on this ratio was evaluated to be about 0.03.

$$\text{ODPA/ODA} = 4A_6/(A_{\text{aromatic}} - 2A_6) \quad (1)$$

where A_6 is the integral of the ODPA H_6 peaks and A_{aromatic}, the integral of the other ODPA and ODA aromatic proton peaks.

A good correlation was found between the theoretical and experimental values (Table 3). As FTIR analysis suggests, the ODPA–ODA oligomers are diamine-terminated and the ODPA–ODA sequence length should be close to the theoretical value reported in Table 3. For all the copolyimides based on ODA, the chemical shift of the *tert*-butyl protons is

Table 1
Synthesized homopolyimides and copolyimides

Acronyms	Diamine	ODPA/BCDA
ODA-0	ODA	100/0
ODA-5	ODA	95/5
ODA-10	ODA	90/10
ODA-20	ODA	80/20
ODA-100	ODA	0/100
ODAOMe-0	ODAOMe	100/0
ODAOMe-5	ODAOMe	95/5
ODAOMe-10	ODAOMe	90/10
ODAOMe-20	ODAOMe	80/20
ODAOMe-100	ODAOMe	0/100
$ODACF_3$-0	$ODACF_3$	100/0
$ODACF_3$-5	$ODACF_3$	95/5
$ODACF_3$-10	$ODACF_3$	90/10
$ODACF_3$-20	$ODACF_3$	80/20
$ODACF_3$-100	$ODACF_3$	0/100

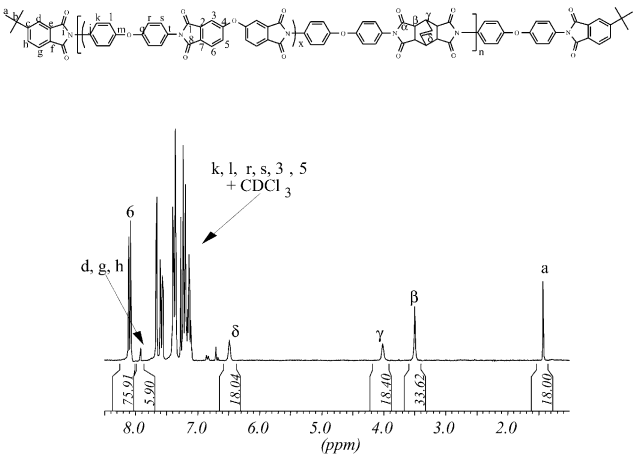

Fig. 2. 250 MHz ^{1}H NMR spectrum of the ODA-20 copolyimide.

Table 2
Characteristics of ODPA/BCDA copolyimides determined by proton NMR

Acronyms	Molar content of BCDA (%)	M_n (g/mol)
ODA-0	0	21,000 ± 2,000
ODA-5	5.1 ± 0.5	19,800 ± 800
ODA-10	10.2 ± 0.5	22,000 ± 1,000
ODA-20	19.9 ± 0.8	21,000 ± 1,000
ODA-100	100	16,400 ± 400
ODAOMe-0	0	20,000 ± 200
ODAOMe-5	5.0 ± 0.5	20,200 ± 700
ODAOMe-10	10.0 ± 0.5	21,000 ± 1,000
ODAOMe-20	19.7 ± 0.1	22,000 ± 1,000
ODAOMe-100	100	20,500 ± 700
$ODACF_3$-0	0	21,000 ± 800
$ODACF_3$-5	4.9 ± 0.3	20,000 ± 900
$ODACF_3$-10	10.0 ± 0.2	20,000 ± 300
$ODACF_3$-20	20.2 ± 0.6	20,200 ± 600
$ODACF_3$-100	100	21,000 ± 1,000

1.456 ± 0.003 ppm, i.e. the same than the BCDA–ODA and ODPA–ODA homopolyimides. Based on these results, it seems reasonable to consider that the copolyimide macromolecular structure is close to the predicted one, i.e.

PAtBu–[(ODA–ODPA)$_x$–ODA–BCDA–]$_n$–ODA

–(ODPA–ODA)$_x$–PAtBu

3.3.2. Copolyimides based on the ODAOMe diamine

For the oligomers based on the ODA diamine, the FTIR spectrum of ODPA–ODAOMe oligomers shows characteristic peaks of both the imide rings and the diamine functions. Moreover, no peak at 1850 cm^{-1}, characteristic of the ODPA anhydride function, was observed. Fig. 3 gives the NMR spectrum of ODAOMe-20 oligomers along with the proton assignments. Apart from the aromatic resonance domain, an interesting part of the spectrum around 3.5 ppm is related to the methoxy proton. Indeed, the molar ratio of ODPA to ODAOMe can be calculated using the following relation:

$$\text{ODPA/ODAOMe} = 3A_6/2A_{CH3} \quad (2)$$

where A_{CH3} is the integral of methoxy protons.

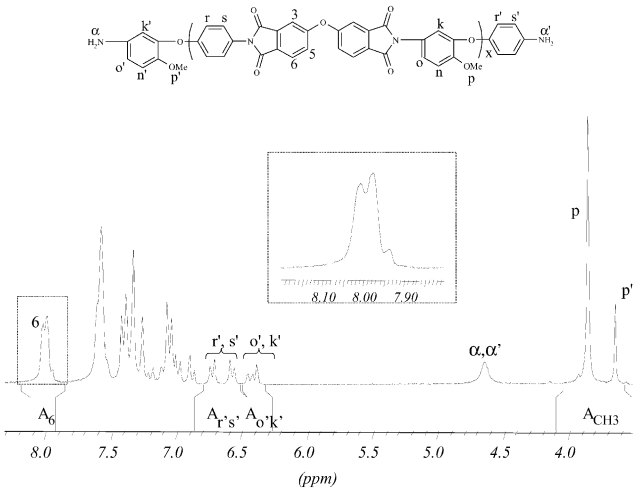

Fig. 3. 250 MHz ^{1}H NMR spectrum of the ODAOMe-20 oligomer.

The experimental values are slightly higher than the theoretical ones, except for ODAOMe-20 oligomer.

Figs. 4 and 5 show the ^{1}H NMR spectra of polyimides, both in the 4.2–3.8 and 1.47–1.42 ppm chemical shift ranges. These NMR signals are assigned to the methoxy and the *tert*-butyl protons, respectively. For both homopolyimides, the methoxy group leads to only one peak at 3.92 ppm for ODAOMe-100 and at 4.01 ppm for ODAOMe-0, while the wide signal at 4.02 ppm for ODAOMe-100 originates from the H_β of the BCDA fragments. The signal at 4.01 ppm could be attributed to the methoxy group of a diamine bounded with two OPDA while the signal at 3.92 ppm could be related to the methoxy group for the BCDA–ODAOMe–BCDA sequence (Fig. 6). For copolyimides, two additional peaks were observed at 3.98 and 3.95 ppm which could be explained by the possibility of two chemical environments for the methoxy group in a BCDA–ODAOMe–ODPA sequence (Fig. 6). The presence of a peak at 3.92 ppm implies that copolyimides also contain BCDA–ODAOMe–BCDA sequences, especially the ODAOMe-20 polymer. These observations are in agreement with the four ^{13}C NMR peaks of methoxy group. Nevertheless, no additional information about the chemical sequence can be inferred from the ^{13}C NMR spectra because attribution of ^{13}C NMR peaks is too ambiguous.

Table 3
Characteristics of diamine-end-capped oligomers

	Acronyms	ODPA/diamine		Molecular length (x)	R
		Theory	Experiment		
Polymer	ODA-0	0.98	0.96		
Oligomers	ODA-5	0.93	0.90	12.6	*
	ODA-10	0.88	0.91	7.3	*
	ODA-20	0.78	0.75	3.6	*
Polymer	ODAOMe-0	0.98	0.97		
Oligomers	ODAOMe-5	0.93	0.96	12.6	0.93 ± 0.11
	ODAOMe-10	0.88	0.91	7.3	0.93 ± 0.02
	ODAOMe-20	0.78	0.90	3.6	0.96 ± 0.05

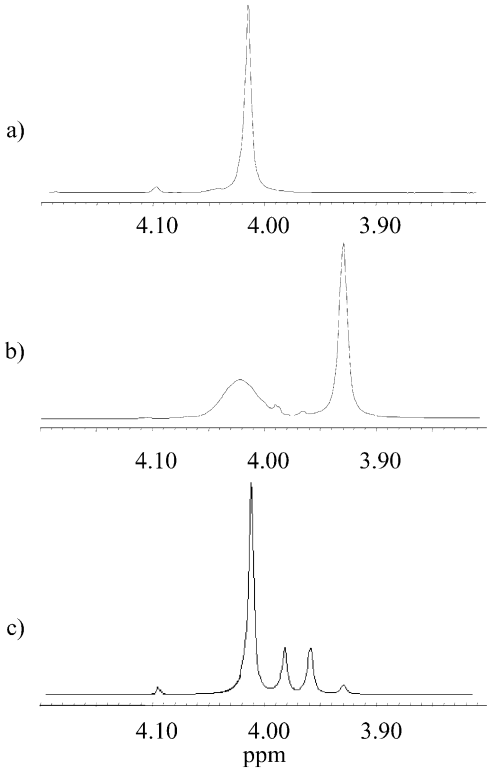

Fig. 4. 400 MHz ^{1}H NMR spectra of: (a) ODAOMe-0, (b) ODAOMe-100, (c) ODAOMe-20 (region of methoxy protons).

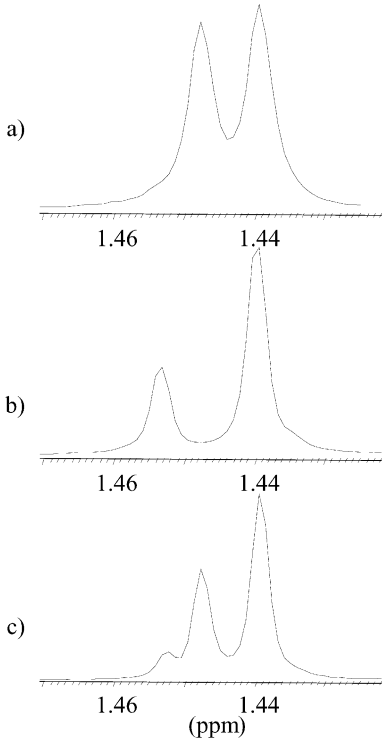

Fig. 5. 400 MHz ^{1}H NMR spectra of tertiobutyl end groups for: (a) ODAOMe-0, (b) ODAOMe-100, (c) ODAOMe-20.

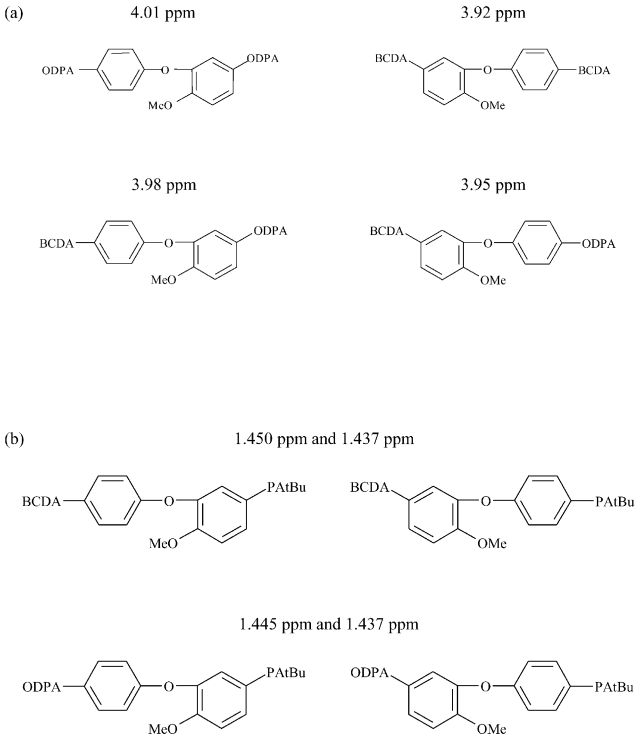

Fig. 6. The possible chemical sequences with the corresponding chemical shift: (a) for methoxy protons, (b) for tertiobutyl protons.

As can be seen in Fig. 5, the protons of the *tert*-butyl end-groups lead to two peaks for the homopolyimides based on the ODAOMe diamine (Table 4). For each homopolyimide, the presence of two well-defined peaks means that it is possible to distinguish both PAtBu–ODAOMe links. For copolyimides, three peaks can be distinguished. It worth noting the presence of a small peak at 1.450 ppm, which suggests the presence of PAtBu–ODAOMe–BCDA sequences for ODAOMe-10 and ODAOMe-20, which were not expected considering the conditions of synthesis.

To account for this phenomenon, we first assumed a possible transimidization reaction between the BCDA monomer and the oligoimides based on ODPA and ODAOMe. Such a reaction has already been mentioned in many papers [18,19] but it usually involves a polyimide chain and an amine function. To confirm our hypothesis, we have mixed a bisimide model compound based on ODPA and 4-fluoroaniline with the BCDA monomer in *m*-cresol for 5 h at 180 °C. The reaction mixture was analyzed by ^{19}F NMR but no evidence of transimidization was found. Indeed, no new resonance peak of ^{19}F due to an imide structure BCDA–fluoroaniline was observed. Another speculative explanation is the presence of free diamine ODAOMe monomers after the first step. This could explain the presence of a shoulder on the H_6 NMR signal at 7.94 ppm for the ODPA–ODAOMe oligomers (Fig. 3) which amounts to about 2% for ODAOMe-20, 0.5% for ODAOMe-10 and 0.2% for ODAOMe-5 oligomers.

Table 4
^{1}H chemical shifts and relative areas of ODAOMe-copolyimides

Acronyms	Integral value of peaks at						
	1.450 ppm	1.445 ppm	1.437 ppm	4.01 ppm	3.98 ppm	3.95 ppm	3.92 ppm
ODAOMe-0		0.50	0.50	1			
ODAOMe-5		0.43	0.57	0.930	0.034	0.035	0.001
ODAOMe-10	0.04	0.39	0.57	0.881	0.051	0.064	0.004
ODAOMe-20	0.05	0.34	0.61	0.690	0.138	0.145	0.027
ODAOMe-100	0.28		0.72				1

Moreover, this hypothesis could be confirmed by the high experimental value of ODPA/ODA ratio found for the ODAOMe-20 copolyimide.

The integration of the r′, s′, o′, k′ and p′ signals (Fig. 3) allows the determination of the aniline end groups/methoxy aniline end groups molar ratio (R) in the oligomers from the following equation:

$$R = 6A_{r's'}/[4(3A_{k'o'} + 2A_{p'})] = 3A_{r's'}/[4A_{p'}] = 2A_{r's'}/[4A_{k'o'}] \quad (3)$$

The R values obtained for the different oligomers are close to 1 (Table 3). Furthermore, the ^{1}H NMR copolyimide analyses show that the molar fractions of both chemical ODPA–ODAOMe–BCDA structures are quite similar (Table 4). In addition, the fractions of both PAtBu–ODAOMe–ODPA sequences are equal while the ratio is 30/70 in the BCDA case (Table 4). It can be concluded that the BCDA dianhydride preferentially reacts with one of the amine function of the ODAOMe monomers. In contrast, the probability that the aniline or the methoxy-aniline functions of ODAOMe react with ODPA is quite equivalent.

3.3.3. Copolyimides based on the $ODACF_3$ diamine

In this case, the ^{1}H NMR spectra of polyimides only show one peak in the *tert*-butyl proton region at 1.46 ppm, irrespective of the polymer. On the other hand, the ^{19}F NMR analyses of the $ODACF_3$ copolyimides give complex spectra (Fig. 7). Two peaks can be distinguished for homopolyimides (Table 5). From the average molecular weight, the molar fraction of the diamines linked to one PAtBu, $X_{ODACF3-PAtBu}$, can be evaluated (Table 5). By comparing these values to the relative areas of the ^{19}F NMR peaks, the small NMR signal could be attributed to the PAtBu–$ODACF_3$–dianhyride sequence while the main peak could be assigned to the other sequences, namely dianhydride–$ODACF_3$–dianhydride.

For the $ODACF_3$-10 and $ODACF_3$-20 systems, four and five peaks can be distinguished, respectively. The main peak at −65.00 ppm could be attributed to ODPA–$ODACF_3$–ODPA and the peak at −65.03 ppm to PAtBu–$ODACF_3$–ODPA sequences. Likewise, the peak at −65.01 ppm can be assigned to the ODPA–$ODACF_3$–BCDA sequences while the peak at −65.13 has not been clearly attributed to one of the other possible sequences. The signal at −65.15 ppm observed for $ODACF_3$-20 could arise from the BCDA–$ODACF_3$–BCDA sequences. These hypotheses are in good agreement with the BCDA molar fraction. Based on these results, we can thus consider that the average number of diamines linked with two BCDA fragments is slightly higher than one per chain, for the $ODACF_3$-20 polymer.

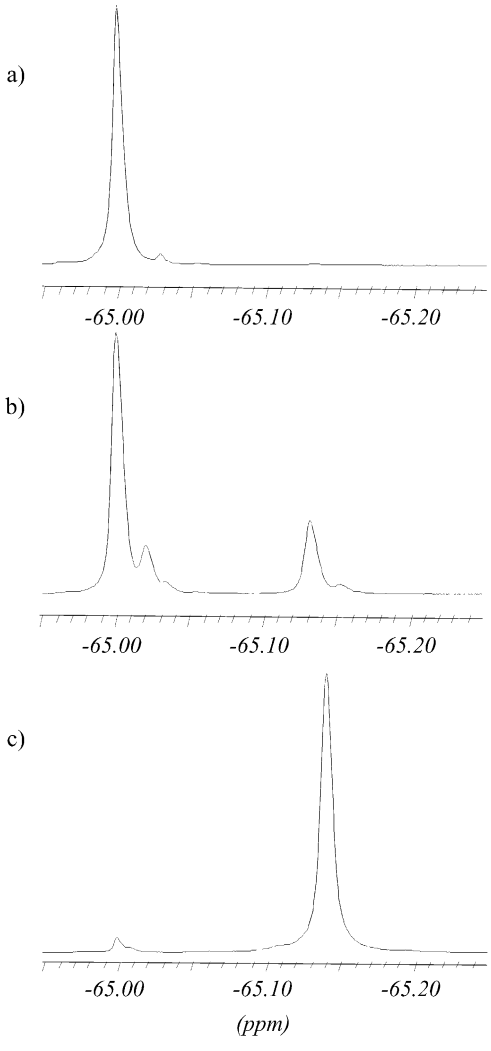

Fig. 7. 400 MHz ^{19}F NMR spectra of: (a) $ODACF_3$-0, (b) $ODACF_3$-20, (c) $ODACF_3$-100.

Table 5
^{19}F Chemical shifts and relative areas of $ODACF_3$-copolyimides

Acronyms	$X_{ODACF3-PAtBu}$[a]	δ (ppm) (relative area)					
$ODACF_3$-0	0.053	− 65.00 (0.980)		− 65.03 (0.020)			
$ODACF_3$-10	0.054	− 65.00 (0.826)	− 65.01 (0.049)	− 65.03 (0.018)	− 61.13 (0.107)		
$ODACF_3$-20	0.053	− 65.00 (0.645)	− 65.01 (0.095)	− 65.03 (0.018)	− 65.13 (0.212)		− 65.15 (0.030)
$ODACF_3$-100	0.048	− 65.00 (0.035)				− 65.14 (0.965)	

[a] The accuracy of the value is 0.002.

Table 6
Solubility ((−) insoluble, (±) partially soluble/swelling, (+) soluble upon heating, (+ +) soluble at room temperature) of copolyimides ODPA/BCDA

Acronyms	Acetone	*m*-cresol	$CHCl_3$	DMF	DMSO	DMAc	NMP	THF
ODA-0	−	++	±	±	–	±	±	−
ODA-5	−	++	±	+	–	±	++	−
ODA-10	−	++	±	+	−	±	++	−
ODA-20	−	++	±	++	±	±	++	−
ODA-100	−	++	−	++	++	++	++	−
ODAOMe-0	−	++	++	+	±	++	++	−
ODAOMe-5	−	++	++	+	+	++	++	−
ODAOMe-10	−	++	++	++	++	++	++	−
ODAOMe-20	−	++	++	++	++	++	++	−
ODAOMe-100	−	++	+	++	++	++	++	−
$ODACF_3$-0	−	++	++	++	±	++	++	++
$ODACF_3$-5	−	++	++	++	++	++	++	++
$ODACF_3$-10	−	++	++	++	++	++	++	++
$ODACF_3$-20	−	++	++	++	++	++	++	++
$ODACF_3$-100	++	++	+	++	++	++	++	++

3.4. Solution properties

The solubility results of copolyimides in some common organic solvents are reported in Table 6. All the synthesized polymers are soluble at room temperature in *m*-cresol. Except for the ODA-0 homopolymer, the other polyimides are also soluble in NMP. At a first glance, we can consider that increasing the BCDA content improves the solubility of the polymers in polar aprotic solvents such as DMSO, DMF and DMAc. These results are in agreement with those reported by Chun [11]. On the contrary, the solubility in chloroform tends to decrease slightly for the BCDA homopolyimide series. It is worth mentioning the beneficial effect of the diamine substituents on the solubility. Indeed, the ODAOMe and $ODACF_3$ polyimides were soluble in more number of solvents than ODA polyimides. Such an enhancement of the solubility could be attributed to the chain distortion induced by the pendent group.

Table 7
Characterizations of copolyimides

Acronyms	Inherent viscosity [η] (dl/g)	T_g (°C)[a]	T_d (°C)	
			N_2	Air
ODA-0	0.683	244	519	488
ODA-5	0.616	248	487	479
ODA-10	0.712	262	492	450
ODA-20	0.572	266	432	432
ODA-100	0.372	384	405	396
ODAOMe-0	0.325	239	425	406
ODAOMe-5	0.369	241	430	416
ODAOMe-10	0.321	241	416	408
ODAOMe-20	0.339	249	408	403
ODAOMe-100	0.457	310	403	388
$ODACF_3$-0	0.526	251	503	451
$ODACF_3$-5	0.544	248	499	463
$ODACF_3$-10	0.435	255	503	466
$ODACF_3$-20	0.383	261	433	423
$ODACF_3$-100	0.212	330	403	406

[a] The accuracy of the T_g value is 2 °C.

The NMP was chosen to determine the intrinsic viscosity of the polyimides (Table 7). The intrinsic viscosities are in the range of 0.320–0.712 dl/g except for $ODACF_3$-100. These values are significantly lower than those mentioned for the BCDA–ODA homopolyimide [11] and of the same order of the magnitude than the reported values for 28,000 g/mol ODPA–ODA [15].

3.5. Thermal properties

The thermal properties of the copolyimides were evaluated by differential scanning calorimetry (DSC) under nitrogen at 20 °C/min. Results are given in Table 7.

Excepted for ODA-100, the glass transition temperatures (T_g) range from 239 to 266 °C. The T_g of the homopolyimide ODA-100 is significantly higher than that for other polyimides. Our results for homopolyimides are consistent with the data in the literature [11,13–15,20]. For all the copolymers under study, the higher the content of BCDA is, the higher the T_g is. This could be related to a certain extent to a decrease in the flexibility of the chains induced by the rigidity of the BCDA structure. On the other hand, the lower T_g of the copolyimides based on ODAOMe could be explained by considering the *meta–para* links favorable for chain flexibility in these specific systems whereas ODA and $ODACF_3$ have a *para–para* structure. However, the difference in the T_g as a function of the diamine depends on the BCDA content.

Thermal gravimetric analyses (TGA) were performed to evaluate the thermal stability of the synthesized polyimides. The TGA thermograms were used to determine the degradation temperatures (T_d) corresponding to a 5%-weight loss (Table 7). The degradation temperature of copolyimides appears within a wide range of temperature. The thermal stability decreases when ODPA is replaced by a BCDA fragment. This could be explained by the retro Diels–Alder reaction of the alicyclic segments [11,12]. Moreover, TGA data suggest that introduction of CF_3 or OMe substituents lowers the thermal stability of the polymers with respect to ODA polyimides.

4. Conclusions

Copolyimides based on the ODPA and BCDA dianhydrides were synthesized using a one pot two-step method of polycondensation with PatBu as an end-capped monomer in order to obtain polyimides with a controlled molecular weight. However, both ^1H and ^{19}F NMR analyses show evidence of some structure defaults with respect to the expected chain structure.

Both thermal and solubility properties of ODPA/BCDA copolyimides depend on the chemical structure of the diamine monomer and on the BCDA content.

As expected, the introduction of trifluoromethyl groups along the polymer backbone noticeably increases the solubility in common solvents without much effect on the thermal stability. On the other hand, we observe an increase in the T_g with the BCDA content, albeit to a smaller extent, as far as methoxy containing polyimides are concerned.

References

[1] Ghosh MK, Mittal KL. Polyimides fundamentals and applications. New York: Marcel Dekker, 1996.
[2] Marek Jr M, Schneider B, Hlavata D, Labsky J, Bleha MJ. Macromol Sci Pure Appl Chem 1996;A33(4):477–89.
[3] Yi MH, Huang W, Choi KY. Pure Appl Chem 1998;12:2009–22.
[4] Kim J-H, Lee S-B, Kim SY. J Appl Polym Sci 2000;77:2756–67.
[5] Chun B-W. J Polym Sci, Polym Phys Ed 1995;33:731–7.
[6] Kim IC, Tak TM. J Appl Polym Sci 1999;74:272–7.
[7] Shiang WR, Woo ED. J Polym Sci Part A: Polym Chem 1993; 31:2081–91.
[8] Rhee SB, Park JW, Moon BS, Lee MH. Macromol Chem Phys 1995; 196:691–704.
[9] Yang C-P, Chen R-S. J Polym Sci Part A: Polym Chem 2000;38: 2082–90.
[10] Yang C-P, Hung K-S, Chen R-S. J Polym Sci Part A: Polym Chem 2000;38:3954–61.
[11] Chun BW. Polymer 1994;35:4203–8.
[12] Itamura S, Yamada M, Tamura S, Matsumoto T, Kurosaki T. Macromolecules 1993;26:3490–3.
[13] Bas C, Albérola ND, Tamagna C, Pascal T. CR Acad Sci-Série IIb 1999;t. 327:1095–100.
[14] Chung IS, Kim SY. Macromolecules 2000;33:3190–3.
[15] Mhaske SB, Bhingarkar RV, Sabne MB, Mercier R, Vernekar SP. J Appl Polym Sci 2000;77:627–35.
[16] Cella JA. Degradation and stability of polyimides. In: Ghosh MK, Mittal KL, editors. Polyimides fundamentals and applications. New York: Marcel Dekker, 1996. p. 343–65.
[17] Tamagna C, Mison P, Pascal T, Petiaud R, Sillion B. Polymer 1999;40:5523–30.
[18] Bender TP, Wang ZH. J Polym Sci, Part A: Polym Chem 2000; 38:3991–6.
[19] Andre S, Guida-Pietrasanta F, Rousseau A, Boutevin B, Caporicio G. J Polym Sci, Part A: Polym Chem 2000;38:2993–3003.
[20] Li Y, Wang X, Ding M, Xu J. J Appl Polym Sci 1996;61:741–8.